METALS AND MATERIALS International, Vol. 12, No. 3 (2006), pp. 207~212

Formation of Amorphous Phase in the Binary Cu-Zr Alloy System

O. J. Kwon[1,2], Y. C. Kim[1], K. B. Kim[1], Y. K. Lee[2], and E. Fleury[1,*]

[1]Advanced Metals Research Center, KIST,
39-1, Hawolgok 2-dong, Seongbuk-gu, Seoul 130-650, Korea
[2] Dept. Metallurgical Engineering, Yonsei University,
134, Sinchon-dong, Seodaemun-gu, Seoul 120-749, Korea

The aim of this work is to elucidate the formation of the amorphous phase in the Cu-Zr binary alloy system. It was found that 1 mm diameter rods with a fully amorphous structure can be prepared in a relatively wide range of compositions. In contrast, the formation of 2 mm diameter rods was achieved only for the $Cu_{64}Zr_{36}$ alloy and in the range of $Cu_{53}Zr_{47}$ - $Cu_{50}Zr_{50}$, which are compositions near the energetically stable Cu_2Zr and CuZr intermetallic compounds. The difference between the calculated Gibbs free energy of the amorphous phase and the intermetallic compounds gives insight into the range of glass formation. In addition, the formation of the energetically stable phases can be kinetically by-passed owing to the crystallization of several competing phases.

Keywords: Cu-Zr alloy, metallic glass, intermetallic compound, thermodynamics

1. INTRODUCTION

Following the discovery by Klement, Willens, and Duwez [1], a large number of metallic amorphous alloys has been prepared by rapid solidification from either a vapor or through melting using techniques such as vapor co-deposition, melt-spinning, splat quenching, laser ablation, or thermal spray deposition. However it has also been demonstrated that the formation of an amorphous phase does not necessarily require a high cooling rate, and can be achieved using various processing methods such as a solid-gas reaction [2], a solid-solid reaction [3,4], ion implantation and irradiation [5], electrodeposition [6], or mechanical alloying [7]. Consequently, it is no longer correct to advance that the amorphous state corresponds to a kinetically frozen liquid. Indeed, Cahn and Bendersky have even proposed that some glassy alloys, which they termed Q-glasses, can nucleate and grow from the melt through a first-order transition [8]. Thus, the amorphous phase formation appears to result from a thermodynamic driving force; i.e., its free energy is lower than that of crystalline phase' as demonstrated for the glass formation in the diffusion couple Au-La [3] and the reverse-melting in Ti-55 %Cr alloy [9]. While the rate can be controlled by the kinetic, the formation of the amorphous phase seems to obey the law of thermodynamics [10,11].

Although the formation of the amorphous phase was reported as early as 1968 in a wide composition range of the binary Cu-Zr alloy system with high solidification rates [12], the synthesis of 1.5 and 2 mm diameter rods with a fully amorphous structure was achieved only recently [13-15]. Due of the limited number of constituent elements, this binary metallic glass provides a new opportunity for experimental and fundamental investigations of the amorphous phase formation, stability, atomic structure and properties.

A study on the formation of the amorphous phase through a suction casting technique was thus undertaken in the composition range of $Cu_{40}Zr_{60}$ - $Cu_{70}Zr_{30}$. In this paper, the composition range of the amorphous phase formation in 1 and 2 mm diameter rods is initially reported. Secondly, an attempt is made to explain the amorphous phase formation based on a thermodynamic approach and an analysis of the crystalline phase formation in 3 mm diameter rods.

This article is based on a presentation made in the symposium "The 7th KIM-JIM Symposium & the 3rd International Symposium on nanostructured Materials Technology", held at KINTEX, Ilsan, Korea, October 27-28, 2005 under auspices of the Korean Institute of Metals and Materials, The Japan Institute of Metals and Center for Nanostructured Materials Materials Technology.

*Corresponding author: efleury@kist.re.kr

2. EXPERIMENTAL PROCEDURE

Ingots of nominal compositions of $Cu_{100-x}Zr_x$ (x = 30 to 60 at.%) were prepared by arc melting mixtures of Cu and Zr pieces having a purity of 99.997 and 99.97 %, respectively. The arc melting was performed in a Ti-gettered high purity Ar (99.9999 %) atmosphere. An appropriate amount of each ingot was remelted and then sucked by vacuum pump into copper molds having cylindrical cavities of 1, 2 and 3 mm diameters and 50 mm in length. The thermal properties associated with the glass transition and crystallization for the copper mold cast alloys were determined by means of differential scanning calorimetry (DSC; Perkin Elmer DSC-7) at a constant heating rate of 0.667 K/s.

3. RESULTS

3.1. Glass formation

The thermal properties of the binary alloys prepared in the form of cylindrical rods with diameters of 1 mm were analyzed by DSC, and the traces of seven alloy compositions are presented in Fig. 1. The DSC curves are characterized by a shallow endothermic peak and a pronounced exothermic peak indicative of the existence of the amorphous phase. As shown in Fig. 2, the glass transition temperature, T_g, and crystallization temperature, T_x, decreased as the Zr content increased. The values of T_g and T_x obtained for the 1 mm diameter specimens are in agreement with those of splat quenched specimens and melt-spun ribbons [16-19].

In order to check whether the 1 mm diameter rods were fully amorphous or partially crystallized, values of the enthalpy

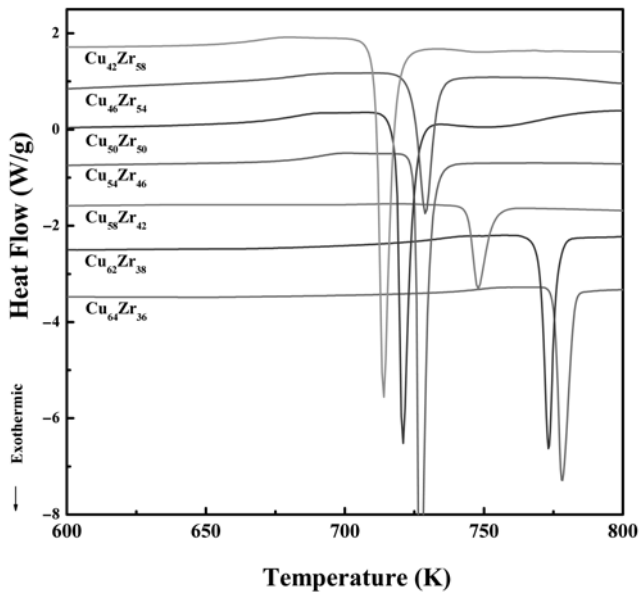

Fig. 1. DSC traces of the ∅1 mm rods for compositions ranging from $Cu_{40}Zr_{60}$ to $Cu_{66}Zr_{34}$.

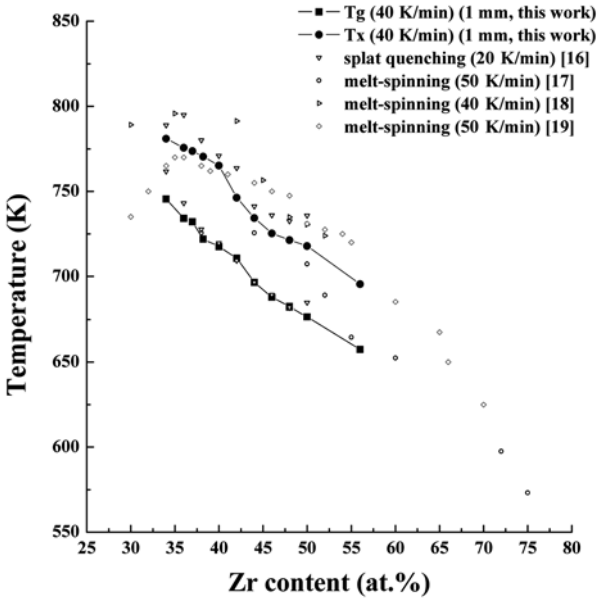

Fig. 2. Variation of the glass transition and crystallization temperature with the Zr content.

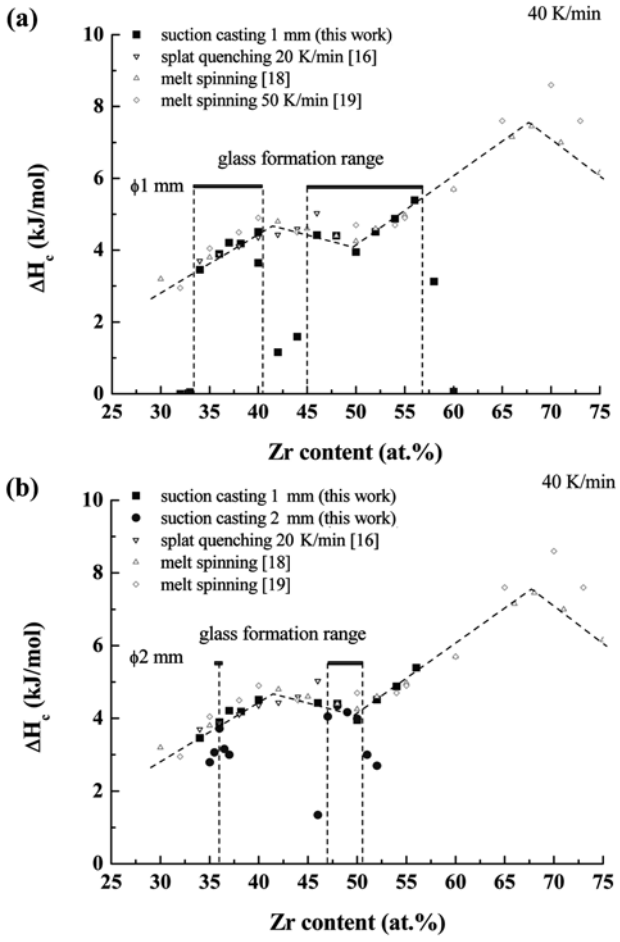

Fig. 3. Variation of the enthalpy of crystallization measured from the ∅1 mm and ∅2 mm rods and a comparison with those obtained from rapidly quenched alloys.

of crystallization obtained from the DSC measurements of the rods were compared with those of the melt-spun ribbons. Figure 3(a) shows that, for most compositions, the values of the enthalpy of crystallization as measured from the 1 mm diameter rods are identical to those measured from the melt-spun ribbons or splat quenched alloys [16,18,19], indicating that these compositions resulted in the formation of 1 mm diameter rods with a fully amorphous structure. However, for a small number of compositions, particularly in the range $Cu_{59}Zr_{41}$ - $Cu_{56}Zr_{44}$, the measured enthalpy of crystallization, ΔH_x, for the 1 mm rods was significantly lower than that for the rapidly quenched alloys, indicating that these specimens were not fully amorphous. To summarize, the formation of the amorphous phase in the 1 mm diameter rods occurred in the composition ranges $Cu_{66}Zr_{34}$ - $Cu_{60}Zr_{40}$ and $Cu_{55}Zr_{45}$ - $Cu_{43}Zr_{57}$.

As shown in Fig. 3(b), the range of composition leading to the formation of the fully amorphous phase in 2 mm diameter rods was found to be significantly reduced. Only the alloys with the composition of $Cu_{64}Zr_{36}$ and those with compositions between $Cu_{57}Zr_{43}$ and $Cu_{50}Zr_{50}$ have a glass forming ability high enough to form a fully amorphous structure in 2 mm diameter rods. These compositions include compositions recently reported by Xu *et al.* [14] and Tang *et al.* [15], and values of the T_g, T_x and ΔH_x are in clear agreement with those reported by these authors.

To understand the range of the composition of the amorphous phase, it is important to inspect the phase diagram of this alloy system. To the authors' knowledge, the most recent version of the Cu-Zr system is that proposed by Braga *et al.* [20]. The phase diagram of this binary alloy system is rather complex; it contains three eutectics and ten intermetallic compounds. These compounds are line compounds and the structure of a number of the phases has yet to be fully identified. The experimental data obtained for the 1 mm diameter rods in this study indicates that the amorphous phase can form for compositions near the Cu_2Zr (orthorhombic, undetermined space group) and CuZr (b.c.c. CsCl-type, $Pm\bar{3}m$) and away from the Cu_8Zr_3 (orthorhombic, Pnma), $Cu_{10}Zr_7$ (orthorhombic, Aba2) and Cu_5Zr_8 (orthorhombic, undetermined space group) intermetallic compounds [20]. According to Braga *et al.* [20], a eutectic with the composition $Cu_{51.5}Zr_{48.5}$ exists between the $Cu_{10}Zr_7$ and CuZr phases. In contrast, the formation of the Cu_2Zr is not yet clear, but may result from the decomposition of the orthorhombic $Cu_{24}Zr_{13}$ at temperatures below 1200 K. It is worth noting that both the Cu_2Zr and CuZr compounds are high temperature phases which decompose into Cu_8Zr_3 + $Cu_{10}Zr_7$ below 1100 °C and $Cu_{10}Zr_7$ + Cu_5Zr_8 below 970 °C, respectively. The Cu_8Zr_3 and Cu_5Zr_8 line compounds also decomposed into $Cu_{51}Zr_{14}$ + $Cu_{10}Zr_7$ below 870 °C and $Cu_{10}Zr_7$ + $CuZr_2$ below 945 °C, respectively [20].

3.2. Thermodynamic properties of the binary Cu-Zr alloys

A major problem in the construction of the Gibbs free energy diagram of glass forming alloys is the determination of the thermodynamics functions of the amorphous and crystalline phases. Experimental data for these quantities are scarce, thus approximations have to be used.

During the liquid-to-solid phase transition, the Gibbs free energy change, ΔG, of a binary A-B system can be expressed as:

$$\Delta G = x_A \Delta G_A + x_B \Delta G_B + \Delta G^{mix} \tag{1}$$

where x_i is the concentration of the element i (i = A, B), ΔG_i is the excess free energy change and ΔG^{mix} is the Gibbs free energy of mixing. ΔG_i can be written as:

$$\Delta G_i = \Delta H_i - T\Delta S_i \tag{2}$$

where ΔH_i, ΔS_i and T are the excess enthalpy, excess entropy and temperature, respectively. The excess enthalpy and excess entropy quantities can be expressed as a function of the specific heats at constant pressure, $C_{P,i}^{A}$, and its evolution as a function of the temperature:

$$H_i^l - H_i^s = \Delta H_{f,i} - \int_T^{T_{f,i}} (C_{P,i}^l - C_{P,i}^s) dT \tag{3}$$

and

$$S_i^l - S_i^s = \frac{\Delta H_{f,i}}{T} - \int_T^{T_{f,i}} (C_{P,i}^l - C_{P,i}^s) \frac{dT}{T} \tag{4}$$

Several expressions have been proposed to estimate the integral terms in Eqs. 3 and 4 that correspond to the difference between the enthalpy and entropy of the undercooled and solid states, respectively. Among these expressions, Perepezko and Paik [21] have shown that the equation proposed by Singh and Holz [22] provides the best approximation. It assumes a linear variation of $\Delta C_{P,i} = C_{P,i}^l - C_{P,i}^s$ with the temperature, which has been experimentally observed [21]. Using the Singh and Holz expression, the Gibbs free energy change becomes:

$$\Delta G = x_a \frac{\Delta H_{f,a}(T_{f,i} - T)}{T_{f,a}} \left(\frac{7T}{T_{f,i} + 6T} \right) + \frac{\Delta H_{f,b}(T_{f,b} - T)}{T_{f,b}} \left(\frac{7T}{T_{f,i} + 6T} \right) + \Delta G^{mix} \tag{5}$$

The Gibbs free energy of mixing, ΔG^{mix}, was calculated according to the formalism thoroughly described by Alonso [23] which is based on the Miedema semi-empirical model [24].

To determine the stability of the amorphous phase in the concentration range of a binary alloy, the Gibbs free energy

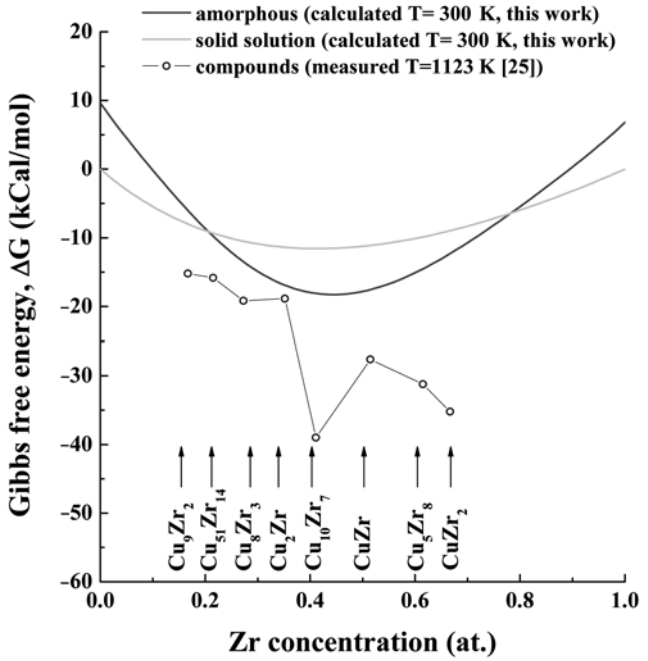

Fig. 4. Calculated Gibbs free energy of the amorphous phase and solid solution, and a comparison with the Gibbs free energy of the intermetallic compounds.

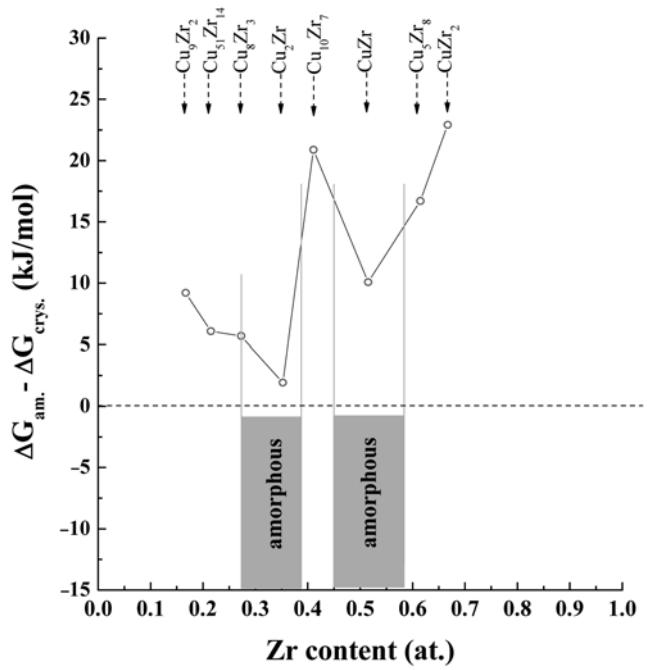

Fig. 5. Difference between the Gibbs free energy of the amorphous phase and the intermetallic compounds, showing the range of the amorphous phase formation.

must be compared with that of the solid solution as well as possible intermetallic compounds.

3.3. Prediction of the glass formation range

Figure 4 shows the calculated dependencies of the Gibbs free energy of the amorphous phase and solid solution at 300 K. In this figure, values of the Gibbs free-energy of the Cu_9Zr_2, $Cu_{51}Zr_{14}$, Cu_8Zr_3, Cu_2Zr, $Cu_{10}Zr_7$, CuZr, Cu_5Zr_8 and $CuZr_2$ intermetallic compounds calculated at 1123K by Zaitsev *et al.* [25] using the associated-solution model are reported for comparison. If the thermodynamic functions of the intermetallic compounds could have been determined at room temperature, the Gibbs free energy would have been lower. With the allowance of the temperature difference, the comparison of the Gibbs free-energy sheds light on the formation range of the amorphous phase in the binary Cu-Zr alloys. The concentration dependencies indicate minimal values of the Gibbs free-energy for the stable $Cu_{10}Zr_7$ and $CuZr_2$ intermetallic compounds. In contrast, Cu_2Zr is characterized by a Gibbs free-energy only slightly lower than that of the amorphous phase. The difference in the Gibbs free-energy between the amorphous and intermetallic compounds is reported in Fig. 5. It is significant that the amorphous phase was found to form experimentally for the composition which has the lowest difference in the Gibb free energy, owing to the strong thermodynamic driving force near the $Cu_{64}Zr_{36}$ alloy composition. In contrast, the

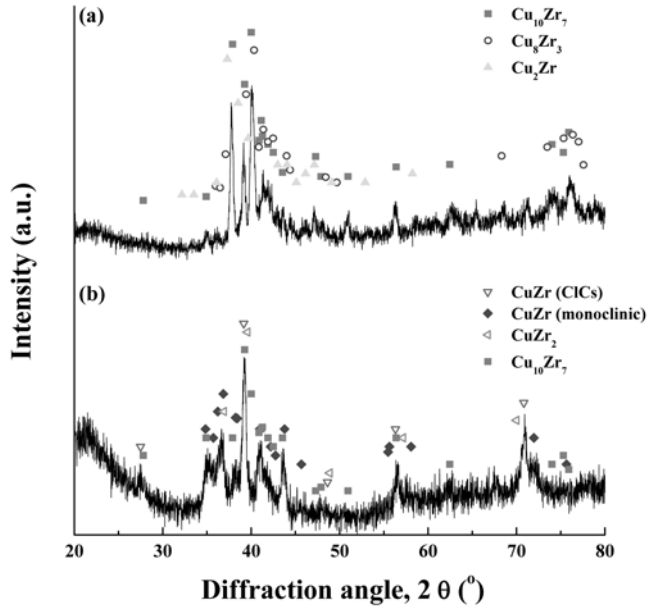

Fig. 6. XRD traces of the 3 mm diameter rods; (a) $Cu_{64}Zr_{36}$ and (b) $Cu_{50}Zr_{50}$ alloys.

Fig. 5 indicates clearly that the amorphous phase will not form for compositions near the stable $Cu_{10}Zr_7$ and $CuZr_2$ intermetallic compounds; both of the Gibbs free-energy values for these compounds are significantly lower than

that of the amorphous phase. However, the thermodynamics cannot explain satisfactorily the formation of amorphous phase near the $Cu_{50}Zr_{50}$ alloy composition. XRD of the 3 mm diameter rods with the $Cu_{64}Zr_{36}$ and $Cu_{50}Zr_{50}$ alloy compositions are presented in Fig. 6(a) and (b), respectively. It is clear that several crystalline phases can be identified. As explained above, the Cu_2Zr phase, stable in the temperature range 1100-1250 K, decomposes into the Cu_8Zr_3 and $Cu_{10}Zr_7$ compounds. These three phases were detected in the XRD of the 3 mm diameter rod of the $Cu_{64}Zr_{36}$ alloy composition (Fig. 6(a)). For the $Cu_{50}Zr_{50}$ alloy, four phases could be identified; the CuZr (B2 structure, CsCl-type), $Cu_{10}Zr_7$ and $CuZr_2$ phases as expected from the phase diagram and, in addition, the metastable monoclinic CuZr (Fig. 6(b)). This metastable monoclinic CuZr phase was not accounted for in the XRD of 5 mm diameter rod of the $Cu_{50}Zr_{50}$ alloy recently reported by Wang *et al.* [26] certainly due to the lower cooling rate. In contrast, upon rapid cooling the decomposition of the CuZr with a B2 structure can induce the formation of the metastable CuZr phase with monoclinic structure (space group $P2_1/m$) that exhibits martensitic characteristics [27]. Consequently, as not a single phase but several phases were found to nucleate and to grow in 3 mm diameter rods with the compositions of $Cu_{64}Zr_{36}$ and $Cu_{50}Zr_{50}$, it can be easily understood that the glass forming ability is also significantly influenced by the crystallization of competing phases. Although the Cu_2Zr and CuZr intermetallic compounds are energetically more stable than the amorphous phase, the formation of these two crystalline phases can easily be bypassed owing to a competing crystallization process, resulting in 2 mm diameter glassy rods for the alloy compositions near $Cu_{64}Zr_{36}$ and $Cu_{50}Zr_{50}$, respectively.

4. SUMMARY

The formation of the amorphous phase in the binary Cu-Zr alloy system was investigated using the suction casting technique. 1 mm diameter rods with a fully amorphous structure were obtained in a wide range of compositions, except for compositions near the Cu_8Zr_3, $Cu_{10}Zr_7$ and Cu_5Zr_8 intermetallic compounds. Glassy rods with diameters of 2 mm were obtained in a narrow composition range near the Cu_2Zr and CuZr phases. The Gibbs free energy diagrams, constructed using the Singh and Holz approximation for the excess energy and the Miedema expression for the mixing enthalpy, provide insight into the formation range of the amorphous phase. However, the relatively large glass formation ability, particularly around the $Cu_{64}Zr_{36}$ and $Cu_{50}Zr_{50}$ alloy compositions, resulted from the competition between the crystallization of several complex intermetallic compounds.

ACKNOWLEDGMENTS

This research was supported by a grant (code #: 05K1501-00510) from the Center for Nanostructured Materials Technology under the '21st Century Frontier R&D Programs' of the Korean Ministry of Science and Technology.

REFERENCES

1. W. Klement Jr., R. H. Willens, and P. Duwez, *Nature* **187**, 869 (1960).
2. K. Samwer and W. L. Johnson, *Phys. Rev. B* **28**, 2907 (1983).
3. R. B. Schwarz and W. L. Johnson, *Phys. Rev. Lett.* **51**, 415 (1983).
4. A. Blatter and M. von Allmen, *Phys. Rev. Lett.* **54**, 2103 (1985).
5. G. Linker, *Solid State Commun.* **57**, 773 (1986).
6. L. Sziraki, E. Kuzmann, M. El-Sharif, C. U. Chisholm, G. Principi, C. Tosello, and A. Vertes, *Electrochem. Commun.* **2**, 619 (2000).
7. R. B. Schwarz, R. R. Petrich and C. K. Saw, *J. Non-Cryst. Solids* **76**, 281 (1985).
8. J. W. Cahn and L. A. Bendersky, *Proc. of Amorphous and Nanocrystalline Metals* (eds. R. Busch, T. C. Hufnagel, J. Eckert, A. Inoue, W. L. Johnson, and A. R. Yavari), Vol. 806, p. MM2.7.1, Materials Research Society, Warrendale, PA, USA (2004).
9. R. Bormann, *Mater. Sci. Eng. A* **178**, 55 (1994).
10. A.L. Greer, *J. Less-Common Met.* **140**, 327 (1988).
11. R. Bormann, *Proc. of Thermodynamics of Alloy Formation* (eds. Y. A. Chang and F. Sommer), p.171, The Minerals, Metals and Materials Society, Warrendale, PA, USA (1997).
12. R. Ray, B. C. Giessen, and N. J. Grant, *Scripta metall.* **2**, 357 (1968).
13. A. Inoue and W. Zhang, *Mater. Trans.* **45**, 584 (2004).
14. D. H. Xu, G. Duan, and W. L. Johnson, *Phys. Rev. Lett.* **92**, 245504-1 (2004).
15. M. B. Tang, D. Q. Zhao, M. X. Pan, and W. H. Wang, *Chinese Phys. Lett.* **21**, 901 (2004).
16. A. J. Kerns, D. E. Polk, R. Ray, and B. C. Giessen, *Mat. Sci. Eng.* **38**, 49 (1979).
17. K. H. J. Buschow, *J. Appl. Phys.* **52**, 3319 (1981).
18. Z. Altounian, Tu Guo-hua, and J. O. Strom-Olsen, *J. Appl. Phys.* **53**, 4755 (1982).
19. E. Kneller, Y. Khan, and U. Gorres, *Z. Metallkd.* **77**, 152 (1986).
20. M. H. Braga, L. Malheiros, F. Castro, and D. Soares, *Z. Metallkd.* **89**, 541 (1998).
21. H. Perepezko and J. S. Paik, *J. Non-Cryst. Solids* **61-62**, 113 (1984).
22. H. B. Singh and A. Holz, *Solid State Commun.* **45**, 985 (1983).
23. J. A. Alonso, L. J. Gallego, and J. M. Lopez, *Philos. Mag. A* **58**, 79 (1988).

24. F. R. de Boer, R. Bloom, W. C. Mattens, A. R. Miedema, and A. K. Niessen, *Cohesion in Metals: Transition Metal Alloys*, North-Holland Physics Publishing, Amsterdam (1989).
25. A. I. Zaitsev, N. E. Zaitseva, Y. P. Alekseeva, S. F. Dunaev, and Y. S. Nechaev, *Phys. Chem. Chem. Phys.* **5**, 4185 (2003).
26. W. H. Wang, J. J. Lewandowski, and A. L. Greer, *J. Mat. Res.* **20**, 2307 (2005).
27. J. W. Seo and D. Schryvers, *Acta mater.* **46**, 1165 (1998).